

Influence of two-level systems on electron phase relaxation in phosphate glasses at low temperatures

A. A. Antipin, B. I. Kochelaev, S. B. Orlinskii, D. A. Fushman, and V. I. Shlenkin

V. I. Ul'yanov-Lenin State University, Kazan'

(Submitted 16 August 1984)

Zh. Eksp. Teor. Fiz. **88**, 1001–1011 (March 1985)

Phase relaxation in activated ytterbium phosphate glasses is investigated by the electron spin echo technique for temperatures between 1.5 and 7 K. Some unusual properties in the phase relaxation process are observed—an exponential decay in the two-pulse echo signal, a linear temperature dependence of the phase relaxation rate of the Yb^{3+} ions, and a residual contribution to the phase relaxation rate which is independent of the Yb concentration and proportional to the stationary magnetic field intensity. It is shown that these features cannot be caused by the Yb^{3+} ions alone. The observed phase relaxation is attributed to the presence of two-level systems characteristic of the amorphous state in the samples investigated.

1. INTRODUCTION

Studies of the physical nature and properties of the amorphous state are becoming important in connection with the wide use of noncrystalline materials in modern technology. Valuable information regarding the microstructure of amorphous materials may be obtained by studying paramagnetic centers and, in particular, rare-earth ions, which are the centers most sensitive to the local ligand fields. However, the large inhomogeneous line broadenings typical of glassy materials make it difficult to deduce this information from EPR spectra recorded under steady-state conditions.¹ A highly sensitive technique employing a laser polarimeter was recently used to observe the EPR spectra of a series of rare-earth and iron-group ions² in phosphate glasses.

In this paper (cf. also Refs. 3, 4) we employ the electron spin echo (ESE) technique for the first time to study phase relaxation of rare-earth ions in glasses. We regard the ESE method as a promising technique for analyzing both the spectral and the dynamic properties of paramagnetic centers in amorphous materials.

2. EXPERIMENTAL RESULTS

We used an ESE spectrometer operating at frequency $\nu \sim 9.4$ GHz in the experiments. The time resolution was 10^{-7} s in the 1.5 to 7 K temperature range and the echo signals were produced by two 50-ns-long rf pulses. The phase relaxation times T_m were deduced from the decay of the ESE signal, and the spin-lattice relaxation time T_1 was found from the recovery of the echo signal after the electronic system was saturated by applying a long pulse of duration ~ 1 ms. The measured relaxation times were accurate to 20%.

We studied phosphate glasses of composition $x\text{Yb}_2\text{O}_3 \cdot (25-x)\text{La}_2\text{O}_3 \cdot 75\text{P}_2\text{O}_5$ with ytterbium contents $x = 0.03, 0.1, \text{ and } 0.3$. The corresponding samples (denoted by I, II, and III) were synthesized from highly purified materials, and the echo signal was reliably observed in all cases. Different types of echo signals (phonon, dipole) have previously been noted in glasses (cf., e.g., the review in Ref. 5). However, paramagnetic centers were clearly responsible for

the echo signal in our experiments; this is apparent both from the vanishing of the echo signal after the constant magnetic field H_0 was turned off and from the absence of echo signals in a sample with a high Yb content $x = 5.0$ (because of the very short phase relaxation times in this sample, ESE signals should indeed not be observed).

We deduced the EPR spectrum of Yb^{3+} from the recorded echo signal by sweeping the magnetic field H_0 . Figure 1 taken from Ref. 3 shows the EPR line for sample I (the relaxation processes were analyzed for $H_0 \approx 2.6$ and 7 kOe); similar spectra were found for samples II and III. The Yb^{3+} ion spin system was responsible for generating the ESE—this is shown convincingly by the dependence of the ESE signal intensity on the Yb content x and by the ratio of the effective g -factors on the weak- and strong-field wings of the EPR line (this ratio was ≈ 4 , which corresponds to the characteristic anisotropy $g_{\perp}/g_{\parallel} \sim 4$ of Yb^{3+} in crystals). The latter result also indicates that the observed EPR signal might be due to random orientations of the local axes of quantization of the Yb^{3+} ions relative to the external magnetic field H_0 .

We observed a nearly exponential decay of the two-pulse echo signal in our experiments. In order to ascertain the nature of the interaction and centers responsible for the loss of coherence among the excited electron spins, we studied the phase relaxation rate T_m^{-1} at the peak of the EPR line ($H_0 = 2.6$ kOe, cf. Fig. 1 in Ref. 3) as a function of the Yb content x . The results in Figs. 1 and 2 show that T_m^{-1} increases linearly with x ; in addition, there is a contribution to T_m^{-1} from the Yb ions which is independent of x . This behavior of $T_m^{-1}(x)$ and the low residual ($x \rightarrow 0$) phase relaxation rate indicate that the Yb^{3+} ions must play a principal role in the dephasing of the electron spins excited by the applied microwave pulses. Following Ref. 6, we will call these type-*A* spins in order to distinguish them from the type-*B* spins, which are not in resonance with the external ac field. The interaction among the Yb^{3+} ions affects the decay of the ESE signal by two mechanisms (instantaneous and spectral diffusion⁶). It was suggested in Ref. 7 that the contributions of these mechanisms might be distinguished by exploiting the characteristic dependence of the rate T_m^{-1} on

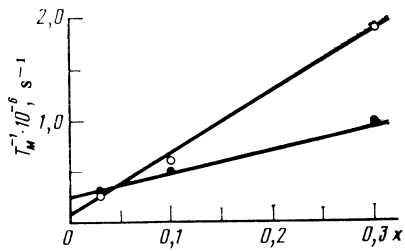


FIG. 1. Phase relaxation rate vs Yb^{3+} ion concentration in phosphate glass at $T = 2$ K: the light and dark circles are for $H_0 = 2.6$ and 7.0 kOe, respectively. The solid curves were calculated from (17) and intersect at the point $x = 0.03$.

the microwave pulse amplitudes for instantaneous diffusion. In our samples, T_m^{-1} did not change significantly when this amplitude was decreased by ~ 10 dB. This indicates that spectral diffusion is dominant in the decay of the ESE signal, which is hardly surprising since the microwave pulses excite only a small portion of the entire EPR line. Spectral diffusion, which involves random changes in the local fields of the A spins caused by flipping of the type- B spins that produce the field, may be caused by spin-lattice relaxation of the B -spins or by changes in their relative orientations. We studied T_m^{-1} and T_1^{-1} as functions of the temperature T (Fig. 2) in order to clarify the role of these processes. A dependence $T_m^{-1} \propto T$ was observed for $1.5 \leq T \leq 5$ K, for which spin-lattice relaxation of the A spins is insignificant; this indicates that the reorientation of the B spins is caused by the spin-lattice relaxation (the samples were of type T_1 , cf. Ref. 6). This is because under our experimental conditions ($\hbar\omega \ll kT$), flip-flop processes should give a temperature-independent contribution to T_m^{-1} . The large inhomogeneous broadening of the EPR spectrum discouraged effective reorientation of the Yb^{3+} ion spins in our experiment. However, even if the Yb^{3+} ions are regarded as type- B spins, their spin-lattice relaxation cannot account for the observed features of the phase relaxation. Indeed, Fig. 2 shows that the different temperature behavior T_1^{-1} for samples I and III is not reflected in any difference in the phase relaxation rates. Furthermore, the measured times T_1 greatly exceed the observed length of the echo signal, which should imply a nonexponential decay law for the spontaneous echo signal^{6,8,9}:

$$v(2\tau) = v_0 \exp(-\alpha\tau^\kappa) \quad (1)$$

with $\kappa = 2$ and a dependence of the form $T_m^{-1} \propto [nT_1^{-1}(T)]^{1/2}$, where n is the concentration of Yb^{3+} ions. However, this conflicts with the observed decay, which is exponential ($\kappa \sim 1$) and for which T_m^{-1} depends linearly on T and n . Departures from exponential decay (values $\kappa > 1$) could be discerned only at the lowest temperature $T < 2$ K for samples II and III.

In order to gain additional information, we studied the phase relaxation process for the maximum magnetic field strengths $H_0 = 7.0$ kOe under our conditions (Fig. 2). The phase relaxation kinetics and the behavior $T_m^{-1}(T)$ were similar to the case for weak fields H_0 . Analysis of the concentration dependence $T_m^{-1}(x)$ (Fig. 1) revealed that the residual value $T_m^{-1}(x = 0)$ on the strong-field wing of the EPR spec-

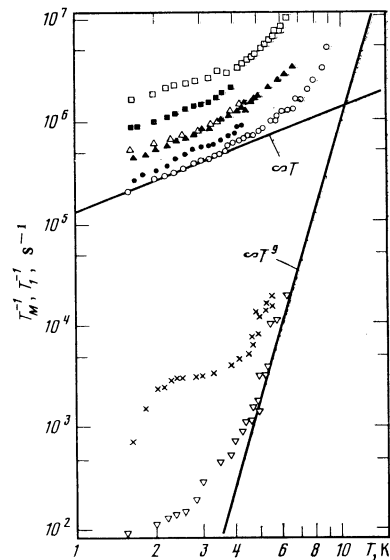


FIG. 2. Temperature dependence of the phase and spin-lattice relaxation rates for Yb^{3+} ions in phosphate glass. The circles, triangles, and squares correspond to samples I, II, and III, and the dark and light figures correspond to magnetic fields $H_0 = 7.0$ and 2.6 kOe, respectively. The values of T_1^{-1} were measured for $H_0 = 2.6$ kOe and are denoted by ∇ and \times for samples I and III, respectively.

trum was larger than for $H_0 = 2.6$ kOe, whereas the increase of T_m^{-1} with x was at least as rapid as for the case of weak fields.

The main features of the phase relaxation process in our glass samples may be briefly summarized as follows: a) the spontaneous ESE signal decays exponentially; b) the phase relaxation rate T_m^{-1} depends linearly on the temperature; c) $T_m^{-1}(x = 0)$ is nonzero; d) the dependence $T_m^{-1}(x)$ is different for strong and weak magnetic fields H_0 . These experimental findings cannot be explained solely in terms of the effects of the Yb^{3+} ions—some additional analysis is required. This analysis will lead us to postulate the presence of fast centers which relax rapidly compared to the Yb^{3+} ions; the fast centers act as type- B spins and dephase the precession of the type- A spins by the spectral diffusion mechanism. We will discuss some specific physical models for the fast centers and the nature of their interaction with the Yb^{3+} ions in the next section.

3. PHYSICAL MODELS FOR THE FAST CENTERS

We will attribute the observed features of the phase relaxation process to the presence of two-level tunnel (TLT) systems in the samples; these systems are characteristic of the amorphous state¹⁰⁻¹² and are responsible for the low-temperature behavior of glasses (Ref. 13).¹¹ The TLT systems consist of two closely spaced low-lying energy levels of an atom or group of atoms moving in a double-well potential (cf. Refs. 12, 15-18 for specific physical models); they are therefore sensitive to the properties of this potential, which are ultimately determined by distortions in the environment surrounding the TLT systems. Both the asymmetry in the double-well potential (the difference in the well energies) and the heights of the barriers separating the wells typically vary widely for glasses.¹⁹ This is reflected in a broad distribution

of the energy difference E between the levels of the TLT systems and in the tunneling parameter λ : E ranges from 0 to several tens of degrees Kelvin, and $0 < \lambda \leq \lambda_{\max} = \eta$ (we write the tunnel splitting in the form $\Delta = Ee^{-\lambda}$). Thermal vibrations of the lattice modulate the asymmetry of the double-well potential and cause transitions between the TLT states; the spin-lattice relaxation rate for a two-level tunnel system (conveniently described in terms of a "spin" $\sigma = 1.2$), is given by^{10,20}

$$R(E, \lambda) = \frac{e^{-2\lambda}}{2\pi\rho\hbar^4} \left(\frac{\gamma_l^2}{v_l^5} + 2 \frac{\gamma_t^2}{v_t^5} \right) E^3 \operatorname{cth} \frac{E}{2kT}, \quad (2)$$

where γ_l, γ_t are the coupling constants of the TLT system with longitudinal and transverse sound, v_l, v_t are the corresponding velocities of sound, and ρ is the density of the material. The spread in the values of E and λ gives rise to a spin-lattice relaxation "spectrum" for the TLT system, and for $E = 2kT$ we readily find that

$$R(2kT, \lambda) \sim 4 \cdot 10^8 T^3 e^{-2\lambda} [\text{s}^{-1}]. \quad (3)$$

Here and throughout the rest of this article we will take $\rho = 4 \text{ g/cm}^3$ and $\gamma_l \approx \sqrt{2}\gamma_t \sim 1 \text{ eV}$ in our numerical estimates and will use the known elastic constants and TLT system parameters for fused quartz.²⁰

Comparison of (3) with the measured values of T_1^{-1} for Yb^{3+} (Fig. 2) implies that the two-level tunnel systems relax rapidly under our experimental conditions. Moreover, the TLT systems play a double role in the phase relaxation process. First, they can act directly as type- B spins and influence the dephasing of the electron spin precessions; second, the interaction of an Yb^{3+} ion present near a TLT system with the latter can convert the Yb^{3+} ion into a rapidly relaxing paramagnetic center, which also acts as a type- B spin. We will analyze both of these mechanisms in detail.

a) Two-level tunnel systems as B spins

Because the lattice deformation depends on which well in the double-well potential contains the localized atom as part of the TLT system, the latter is coupled by the static strain field both with the other TLT systems and with the paramagnetic ions in much the same way as for the analogous interaction among paramagnetic ions.^{21,22} The interwell transitions give rise to a "transverse" interaction component which flips the spin of the TLT system. The coupling among the TLT systems was studied in Refs. 20 and 23; here we will consider the coupling between the TLT systems and the paramagnetic ions. If the distance r between them is large enough so that the elastic model applies, the interaction between the ion and the TLT system via the elastic strain field is described by the Hamiltonian

$$\mathcal{H} = \frac{G}{4\pi\rho v_l^2 r^3} S_z \sigma_z (1 - e^{-2\lambda})^{1/2} \sum_{\alpha} 2\gamma_{\alpha} (1 - 3\zeta_{\alpha}^2), \quad (4)$$

which can be derived as in Refs. 20 and 24 from the equations of elasticity. Here we have written out only the z - z component of the interaction; $\hat{\sigma}$ and \hat{S} are the pseudospin and spin operators for the TLT system and for the ion, respectively (here σ_z , with a prime on the subscript z , denotes the projection of $\hat{\sigma}$ on a fictitious axis z' which does not corre-

spond to any spatial direction); the $\{\gamma_{\alpha}\}$ are the eigenvalues of the coupling tensor, which describes the coupling of the TLT system with the elastic vibrations; the ζ_{α} are the direction cosines of the vector \mathbf{r} relative to the principal axes of the coupling tensor; G is the coupling constant of the ion spin with the lattice (for simplicity we will take the G -tensor to be isotropic). The continuous (elastic) medium approximation does not apply for ions lying close to the TLT systems, and the following microscopic analysis is needed to derive the Hamiltonian. We write the operator for the crystal field generated by the Yb^{3+} ligands in the matrix form

$$\hat{V}_{\text{cr}} = \sum_i \begin{pmatrix} \hat{V}(r_i) & 0 \\ 0 & \hat{V}(r_i') \end{pmatrix}, \quad (5)$$

with respect to a basis given by the two states of the TLT system. Here $\hat{V}(r_i)$ and $\hat{V}(r_i')$ are the contributions from the i th ligand when the latter is localized at points \mathbf{r}_i and \mathbf{r}_i' in different wells of the double-well potential. If we confine our attention to the lower (Kramers) doublet of the Yb^{3+} ion and allow for tunneling, the ion-TLT system interaction is described by the Hamiltonian

$$\mathcal{H}' = (CS_z + DS_x) [\sigma_z (1 - e^{-2\lambda})^{1/2} + \sigma_x e^{-\lambda}], \quad (6)$$

where

$$C = \sum_i (V(r_i) - V(r_i')), \quad D = \sum_i (\hat{V}(r_i) - \hat{V}(r_i')),$$

and \hat{V} also allows for mixing of the higher-lying ionic states by the magnetic field. In contrast to (4) we have retained the transverse-spin component of the Hamiltonian, which will be essential in what follows.

If we now regard the TLT system as a B -spin system and neglect the small fraction of the A -spins that happen to be near the TLT system, we must use (4) as the Hamiltonian for the coupling between the TLT system and the type- A spins. Because the inhomogeneous widths are large for both the EPR and the TLT energy spectra, we may neglect any fortuitous equalities in the energy splitting of the ion and TLT system; we can therefore limit ourselves to the z - z component of \mathcal{H} in analyzing how the phase relaxation process is influenced by spectral diffusion mediated by the interaction of the TLT systems with the A -spins via the elastic strain field (cf. Ref. 8).

b) Indirect effects associated with TLT systems

We now consider a Yb^{3+} ion (denoted by Yb^* in what follows) located near a TLT system; the Hamiltonian for the interaction with the TLT system is given by (6). The transitions between the TLT states caused by the interaction with thermal vibrations rapidly modulate the transverse fields generated by the TLT system at the Yb^* center, thereby providing an additional channel for electron spin relaxation. Similar models were considered in Refs. 25–27 in order to explain the observed features of relaxation in amorphous samples, i.e., to analyze how the transitions in the TLT systems modulate the hyperfine interactions and thereby influence the electron and nuclear quadrupole relaxation in amorphous materials.

A calculation similar to the ones in Refs. 26 and 28

yields the expression

$$R^*(\omega, E, \lambda) = \frac{1 - e^{-2\lambda}}{4\hbar^2 \text{ch}^2(E/2kT)} \left(G \frac{\delta r}{r} \right)^2 \frac{R(E, \lambda)}{\omega^2 + R^2(E, \lambda)} \quad (7)$$

for the spin-lattice relaxation rate for a Yb* center. In order to simplify the estimates, we have replaced

$$\sum_i (\bar{V}(r_i) - \bar{V}(r_i')) \approx \sum_i \frac{\partial \bar{V}(r_i)}{\partial r_i} |r_i - r_i'|$$

by $G^* \delta r/r$, where $G^*(\propto H_0)$ is the spin-lattice coupling constant for Yb*, $\delta r = |r - r'| \ll r$ is the ligand displacement, and $\hbar\omega$ is the splitting of the ion levels. Because of the spread in the parameters E and λ of the TLT systems, the spin-lattice relaxation rates of the Yb* centers acquire a corresponding scatter; for $E = 2kT$, $\delta r/r \sim 0.1$, $\omega/2\pi \sim 9.4$ GHz, and $G^* \sim G \sim 3 \text{ cm}^{-1}$ we obtain²⁾ [using (3)]

$$R^*(\lambda) \sim 4 \cdot 10^7 T^3 e^{-2\lambda} (1 - e^{-2\lambda}) / (1 + 4 \cdot 10^{-5} T^6 e^{-4\lambda}) [\text{s}^{-1}]. \quad (8)$$

Comparison of these estimates with Fig. 2 implies that Yb* is a rapidly relaxing center. Unlike the TLT systems, the Yb* are paramagnetic and are coupled to the A -spins by the dipole-dipole interaction.

For strongly, inhomogeneously broadened EPR lines, most of the Yb^{3+} ions are B -spins; many Yb* centers may therefore be present even though the Yb^{3+} ions have a low probability of being located close to a TLT system. If we assume that the TLT systems and Yb^{3+} ions are uniformly and independently distributed in the sample, the concentration of Yb* centers can be estimated by

$$n^* = 2x\tilde{n}\xi = 0,04n\xi, \quad (9)$$

where the value $\tilde{n} \sim 4 \cdot 10^{18} \text{ cm}^{-3}$ is typical for the concentration of TLT systems with $E \leq 30$ K, n is the concentration of Yb ($\sim 2x \cdot 10^{18} \text{ cm}^{-3}$), and ξ is the fraction of sites in the $25\text{LaO}_2\text{O}_3\text{-}75\text{P}_2\text{O}_5$ "molecule" containing a TLT system (ξ must be high enough so that a Yb^{3+} ion in the same molecule relaxes rapidly). Even though their concentration n is less than \tilde{n} , the Yb* centers are important in the phase relaxation process; this is due in part to their strong coupling with the A -spins, and in part to the fact that the spread in λ causes the strength of the A -spin-TLT interaction to vary and thereby diminishes the influence of the TLT systems on the relaxation.

The TLT systems present in the glasses should thus give rise to two types of fast centers; moreover, because of the wide spread in the spin-lattice relaxation rates under our experimental conditions, there will always exist fast centers of both types for which the spin vector flips only a few times during the lifetime 2τ of the observed echo signal. These fast centers will thus strongly influence the dephasing of the A -spin precessions^{29,30} and cause the spontaneous echo signal to decay exponentially. We will discuss how the fast centers affect the decay of the echo signal in the next section, together with results of numerical calculations of $v(2\tau)$.

4. CALCULATION OF $v(2\tau)$

We can derive an expression for the decay of a two-pulse echo signal by regarding both types of fast centers as B -spins. The echo signal amplitude at time 2τ is given by

$$v(2\tau) = v_0 \left\langle \left\langle \exp \left\{ i \left[\sum_j A_{ij} f_{j\sigma}(2\tau) + \sum_k A_{ik} f_{k\sigma}(2\tau) \right] \right\} \right\rangle \right\rangle_i, \quad (10)$$

where the angular brackets denote an average over all possible configurations, including the distribution of the TLT system parameters and the g -factors of the Yb* ions, and over all possible random changes in the B -spin orientation ($\langle \dots \rangle_i$);

$$A_{ij} = \frac{G_A (1 - e^{-2\lambda})^{1/2}}{4\pi\rho v_i^2 r_{ij}^3 \hbar} \sum_{\alpha} 2\gamma_{\alpha} (1 - 3\xi_{\alpha}^2),$$

$$A_{ik} = \frac{g_A g^* \beta^2}{r_{ik}^3 \hbar} (1 - 3 \cos^2 \theta_{ik}) \quad (11)$$

are the fields produced at an A -spin located at the point r_i by a TLT system and Yb* ion located respectively at r_j and r_k ; $f_{s(\sigma)}$ is defined by

$$f_{s(\sigma)}(2\tau) = \int_0^{2\tau} s(t) m_{s(\sigma)}(t) dt,$$

where $s(t) = 1$ for t in the interval $(0, \tau)$ and $s(t) = -1$ for t in $(\tau, 2\tau)$, and $m_{s(\sigma)}(t)$ is the projection of the spin of Yb* (or of the TLT system) on the z axis (respectively, on the z' axis). Equation (10) neglects the TLT systems responsible for generating the Yb* centers—the fields that they produce at the location of the electron spins are assumed small compared to the dipole fields produced by the Yb*. The dipole fields of the "normal" Yb^{3+} ions have also been omitted in Eq. (10); estimates reveal that because of their slow rate of spin reorientation, their effects on the phase relaxation are minor compared with the influence of the fast centers. We also note that the g -tensor is taken to be isotropic for simplicity, and that the g -factor is assumed to be uniformly distributed in the interval $1 \leq g \leq 4$; a rigorous allowance for the anisotropy and random spatial orientation of the g -tensors should not alter the qualitative results derived below for the electron spins.³¹

In our case, in addition to the standard procedure of averaging over the random spatial positions of the B -spins in a dilute sample (cf., e.g., Refs. 8 and 32), we must also average (10) over the distribution of the parameters of the TLT systems. The spread in the values of E and λ determines the distribution of the spin-flip rates for the fast centers; we will treat it as in Ref. 30, where the influence of spectral diffusion on the decay of phonon echo signals in glass was studied for TLT systems. If we assume the distribution function

$$P(E, \lambda) = P(E) (1 - e^{-2\lambda})^{-1/2}, \quad P(E) = \text{const},$$

for the TLT system parameters³³ and take the spatial position and spin-flip processes for the Yb* ions and TLT systems to be independent, we obtain

$$v(2\tau) = v_0 \exp[-2\Delta\omega_{1/2}(2T)F(\tau) - 2\Delta\omega_{1/2}^*(2T)F^*(\tau)], \quad (12)$$

where the first and second terms in the argument of the exponential are due to the dephasing of the A -spin precessions by the TLT systems and by the Yb* centers, respectively. In Eq. (12), F is defined by

$$F(\tau) = \int_0^{\infty} \frac{dx}{\text{ch}^2 x} \int_{e^{-2\eta}}^1 \frac{dy}{y(1-y)^{1/2}} R(x, y) f(R(x, y)\tau, \text{th } x), \quad (13)$$

$$f(z, \chi) = e^{-z} \int_0^z I_0(\chi(z-z')) (I_0(z') + I_1(z')) z' dz', \quad (14)$$

where we have written $x \equiv E/2kT$ and $y \equiv e^{-2\lambda}$; $I_0(z)$ and $I_1(z)$ are modified Bessel functions; $F^*(\tau)$ is obtained from (13) by replacing $R(x, y) \equiv R(E, \lambda)$ by $R^*(\omega, x, y)$ [cf. (7)], and the quantities

$$\Delta\omega_{1/2}(T) = \frac{4\sqrt{2}\pi^2}{\sqrt{3}\hbar} \frac{G_A 2\gamma_i}{4\pi\rho v_i^2} \frac{kT}{2\eta E_{\max}} \bar{n}', \quad (15)$$

$$\Delta\omega_{1/2}^*(T) = \frac{16\pi^2 g_A g^* \beta^2}{9\sqrt{3}\hbar} \frac{kT}{2\eta E_{\max}} n^*$$

are temperature-dependent, which indicates that the main contribution to the phase relaxation comes from the fast centers generated by TLT systems with splittings $E \leq kT$. We observe that $\hat{n}' = \hat{n} - n^* \approx \hat{n}$ in (15), and we have used the method in Ref. 20 to average over the random orientations of the principal axes of the tensor γ with allowance for the relationship between the $\{\gamma_\alpha\}$ and the measurable quantities γ_i and γ_i^* .

In analyzing the time dependence $v(2\tau)$ it is helpful to write $R(E = 2kT, \lambda) = W e^{-2\lambda}$, where W is the upper bound of the spin-lattice relaxation spectrum for TLT systems with $E \leq 2kT$ (similarly, we can introduce the quantity W^* for³⁾ Yb^* ; however, this is unnecessary because the form of the result remains the same). It is readily shown that $F(\tau) \propto \tau^2$ provided that $W\tau \ll 1$; in this case Eq. (12) reduces to (1) with $\kappa = 2$ (estimates (3) and (8) imply that this will occur for times $\tau \sim 10^{-6}$ s, at least for low temperatures < 1 K). As $W\tau$ increases, some of the B -spins will flip several times during 2τ ($W\tau \gtrsim 1$)—these spins should dephase the precessions of the A -spins most effectively and cause a transition to a phase relaxation kinetics (1) with $\kappa \sim 1$ (Refs. 29, 30). As $W\tau$ rises further, most of the B -spins will eventually satisfy the condition $R(E, \lambda)\tau \gg 1$, so that the decay will be given by (1) with $\kappa \sim 0.5$.

In order to verify the above qualitative conclusions we numerically integrated the expressions for $F(\tau)$ and $F^*(\tau)$, which are shown in Figs. 3 and 4. The calculated values in Fig. 3 confirm the changes in the echo signal decay kinetics noted above as $W\tau$ increases. However, the transition from

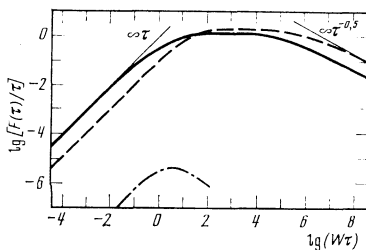


FIG. 3. Curves showing $F(\tau)/\tau$ (solid) and $F^*(\tau)/\tau$ (dashed) as functions of $W\tau$ for $T = 1$ K and $2\eta = 10$. The dashed-and-dotted curve plots $F(\tau)/\tau$ for a system of “normal” spins with fixed values $\lambda = 0$ and $E = 2kT$ (these values were taken from Ref. 29 up to an arbitrary factor).

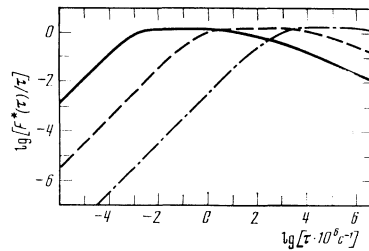


FIG. 4. The dependence of $F^*(\tau)/\tau$ on τ for $2\eta = 10$ for $T = 10$ K, 1 K, and 0.1 K (solid, dashed, and dashed-and-dotted curves, respectively).

$\kappa = 2$ to $\kappa \sim 1$ occurs for $W\tau > 1$ and not for $W\tau \sim 1$, which reflects the influence on the phase relaxation of the numerous TLT systems for which $y \equiv e^{-2\lambda}$ is small [cf. (13)]; this behavior was noted in Ref. 30 (we note parenthetically that the value of $W\tau$ for which the transition to $\kappa \sim 1$ occurs depends on η). The nonzero spread in the reorientation rates for the B -spins makes $F(\tau)/\tau$ considerably larger than is the case for “normal” spins with fixed E and $\lambda = 0$; the values for the latter case are shown by the dashed-and-dotted curve in Fig. 3 (these values were taken up to an arbitrary factor from Ref. 29 for $E = 2kT$; the echo signal was observed to decay exponentially for a time interval 2τ). Figure 4 plots the dependence $F^*(\tau)/\tau$ for three different temperatures [estimate (8) was used for $R^*(\omega, 2kT, \lambda)$]; we see that the fast-center models proposed in Sec. 3 can account for the experimentally observed exponential decay of the echo signal. We note that in spite of the approximate nature of the estimates, the numerical calculation (cf. Fig. 4) also reveals a departure from exponential decay [$\kappa = 1 \rightarrow \kappa > 1$] for $T < 2$ K when $\tau < 1$ μ s; this is in accord with the experimental observations for samples II and III.

If we limit ourselves to the times for which $v(2\tau)$ is exponential, we can write

$$v(2\tau) = v_0 \exp(-\tau T_M^{-1}), \quad (16)$$

$$T_M^{-1} = 2[a\Delta\omega_{1/2}(2T) + b\Delta\omega_{1/2}^*(2T)]. \quad (17)$$

The numerical calculations imply that $a = 1.3$ and $b = 1.55$ for $2\eta = 10$, and Fig. 4 shows that b is independent of T (a similar result is found for a).

5. COMPARISON WITH EXPERIMENT

The linear temperature dependence $T_m^{-1}(T)$ described by Eqs. (15), (17) agrees with the observed behavior of the phase relaxation rate (Fig. 2) for $T < 5$ K. The more rapid increase in T_m^{-1} for $T > 5$ K might be due to an abrupt drop in the spin-lattice relaxation time for the Yb^{3+} ions associated with Raman relaxation processes.

Before discussing the observed features of the concentration dependence $T_m^{-1}(x)$, we first note that the two terms in (17) depend differently on the constant magnetic field H_0 : $\Delta\omega_{1/2} \propto G_A \propto H_0$ (by Kramers' theorem), whereas $\Delta\omega_{1/2}^* \propto g_A = h\nu/\beta H_0$. The first term therefore becomes more important relative to the second as H_0 increases. If we recall that $\Delta\omega_{1/2}^*$ depends linearly on the Yb concentration, we can readily explain the observed behavior $T_m^{-1}(x, H_0)$ [cf. Figs. 1,

2] if the number of TLT systems is assumed to be independent of the Yb concentration in the sample. Comparison of Eq. (17) with the experimental values of T_m^{-1} measured for sample I (with $x = 0.03$) at $T = 2\text{K}$ for two fields H_0 yielded the following values: $\Delta\omega_{1/2} = 0.36 \cdot 10^5 \text{ s}^{-1}$, $\Delta\omega_{1/2}^* = 0.62 \cdot 10^5 \text{ s}^{-1}$ ($H_0 = 2.6 \text{ kOe}$) and $\Delta\omega_{1/2} = 0.97 \cdot 10^5 \text{ s}^{-1}$, $\Delta\omega_{1/2}^* = 0.23 \cdot 10^5 \text{ s}^{-1}$ ($H_0 = 7.0 \text{ kOe}$). We used these values to plot the theoretical curves $T_m^{-1}(x, H_0)$ in Fig. 1. If we take into account the possible errors in measuring T_m^{-1} and the Yb concentration, we see that (17) correctly reproduces the experimentally observed behavior of the phase relaxation rate. We note that the direct effects of the TLT systems on the phase relaxation become important for strong H_0 .

The contributions to T_m^{-1} from both types of fast centers found above were then compared with the approximate values found from (15) by substituting the parameter values typical for fused quartz.²⁰ The theoretical estimate for $\Delta\omega_{1/2}$ was $\approx 180\%$ larger than the experimental value (which is hardly surprising in view of the crudeness of the estimates); as for $\Delta\omega_{1/2}^*$, comparison of the theoretical and experimental curves showed that $n^* \sim 0.1n$, i.e., almost one Yb^{3+} ion in ten relaxed rapidly. Such a high concentration of Yb^* centers [cf. estimate (9)] could conceivably be explained by assuming that a Yb^{3+} ion is converted into a rapidly relaxing Yb^* center whenever it is present together with a TLT system in the same $25\text{La}_2\text{O}_3 \cdot 75\text{P}_2\text{O}_5$ molecule (i.e., $\xi \sim 1$). However, we think it is more likely that the TLT systems tended to cluster around the rare-earth ions while the samples were being fabricated; rare-earth ions are known to disrupt the disordered network of bonds in the glass.³⁴

6. CONCLUSIONS

We have experimentally detected some unusual properties of electron phase relaxation in phosphate glasses activated with ytterbium which may be ascribed to the presence of two-level tunnel systems in the samples. This provides additional confirmation of the importance of TLT systems in the low-temperature behavior of amorphous systems and also demonstrates that the ESE technique can be employed to analyze disordered materials.

We thank S. G. Lunter for synthesizing the samples.

¹⁾We note that the samples probably contained OH^- hydroxide impurities (cf. Ref. 14); however, according to Ref. 15, OH^- groups in oxide glasses can be regarded as "impurity" two-level tunnel systems with properties similar to those for ordinary two-level systems.

²⁾The rough estimates for G were deduced from the Raman relaxation rate $\sim 10^{-3} T^9 \text{ s}^{-1}$ observed in Refs. 2, 3.

³⁾For example, $R^*(\omega, E = 2kT, \lambda) = 4W^*e^{-2\lambda}(1 - e^{-2\lambda})$.

¹⁾D. L. Griscom, *Non-Cryst. Solids* **40**, 211 (1980).

²⁾A. A. Antipin, V. S. Zapasskiĭ, and S. G. Lunter, *Fiz. Tverd. Tela (Leningrad)* **24**, 3248 (1982) [*Sov. Phys. Solid State* **24**, 1843 (1982)].

³⁾A. A. Antipin, B. I. Kochelaev, and V. I. Shlenkin, *Pis'ma Zh. Eksp. Teor. Fiz.* **39**, 155 (1984) [*JETP Lett.* **39**, 182 (1984)].

⁴⁾A. A. Antipin, B. I. Kochelaev, S. B. Orlińskiĭ, D. A. Fushman, and V. I. Shlenkin, in: *Proc. All-Union. Conf. Magnetic Resonance in Condensed Media* [in Russian], Part 1, Kazan' (1984), p. 134.

⁵⁾B. P. Smolyakov and E. P. Khaĭmovich, *Usp. Fiz. Nauk* **136**, 317 (1982) [*Sov. Fiz. Usp.* **136**, 102 (1982)].

⁶⁾J. R. Klauder and P. W. Anderson, *Phys. Rev.* **125**, 912 (1962).

⁷⁾A. M. Raĭtsimring, K. M. Salikhov, B. A. Umanskiĭ, and Yu. D. Tsvetkov, *Fiz. Tverd. Tela (Leningrad)* **16**, 756 (1974) [*Sov. Phys. Solid State* **16**, 492 (1974)].

⁸⁾K. M. Salikhov, A. G. Semenov, and Yu. D. Tsvetkov, *Élektronnoe Spinnovoe Ékko i ego Primenenie (Electron Spin Echoes and their Applications)*, Nauka, Novosibirsk (1976).

⁹⁾P. Hu and S. R. Hartman, *Phys. Rev. B* **9**, 1 (1974).

¹⁰⁾P. W. Anderson, B. I. Halperin, and C. M. Varma, *Philos. Mag.* **25**, 1 (1972).

¹¹⁾W. A. Phillips, *J. Low Temp. Phys.* **7**, 351 (1972).

¹²⁾F. N. Ignat'ev, V. G. Karpov, and M. I. Klinger, *Dokl. Akad. Nauk SSSR* **269**, 1341 (1983) [*Sov. Phys. Dokl.* **269**, 342 (1983)].

¹³⁾W. A. Phillips, ed., *Amorphous Solids: Low-Temperature Properties*, Springer Verlag, New York (1981).

¹⁴⁾S. G. Lunter, A. N. Mironov, and Yu. K. Fedorov, *Fiz. Khim. Stekla* **9**, 364 (1983).

¹⁵⁾W. A. Phillips, *Philos. Mag.* **B43**, 747 (1981).

¹⁶⁾V. G. Karpov, M. I. Klinger, and F. N. Ignat'ev, *Zh. Eksp. Teor. Fiz.* **84**, 760 (1983) [*Sov. Phys. JETP* **57**, 439 (1983)].

¹⁷⁾V. G. Karpov and M. I. Klinger, *Pis'ma Zh. Tekh. Fiz.* **6**, 1478 (1980) [*Sov. Tech. Phys. Lett.* **6**, 636 (1980)].

¹⁸⁾V. G. Karpov and D. A. Parshin, *Pis'ma Zh. Eksp. Teor. Fiz.* **38**, 536 (1983) [*JETP Lett.* **38**, 648 (1983)].

¹⁹⁾P. W. Anderson, in: *Les Houches Lectures on Ill-Condensed Matter*, R. Balian (ed.), North-Holland, New York (1979), p. 162.

²⁰⁾J. L. Black and B. I. Halperin, *Phys. Rev. B* **16**, 2879 (1977).

²¹⁾K. Sugihara, *J. Phys. Soc. Jpn.* **14**, 1231 (1959).

²²⁾L. K. Aminov and B. I. Kochelaev, *Zh. Eksp. Teor. Fiz.* **42**, 1303 (1962) [*Sov. Phys. JETP* **15**, 903 (1962)].

²³⁾J. Joffrin and A. Levelut, *J. Phys. (Paris)* **36**, 811 (1976).

²⁴⁾N. M. Galeeva and B. I. Kochelaev, *Fiz. Tverd. Tela (Leningrad)* **19**, 1354 (1977) [*Sov. Phys. Solid State* **19**, 787 (1977)].

²⁵⁾M. K. Bowman and L. Kevan, *J. Phys. Chem.* **81**, 456 (1977).

²⁶⁾S. R. Kurtz and H. J. Stapleton, *Phys. Rev. B* **22**, 2195 (1980).

²⁷⁾J. Szeftel and H. Alloul, *J. Non-crystal. Solids* **29**, 253 (1978).

²⁸⁾A. Abragam, *The Principles of Nuclear Magnetism*, Clarendon Press, Oxford (1961).

²⁹⁾P. Hu and L. R. Walker, *Phys. Rev. B* **18**, 1300 (1978).

³⁰⁾P. Hu and L. R. Walker, *Solid State Comm.* **24**, 813 (1977).

³¹⁾A. G. Maryasov, S. A. Dzuba, and K. M. Salikhov, *J. Magn. Res.* **50**, 432 (1982).

³²⁾W. B. Mims, "Electron spin echoes," in: *Electron Paramagnetic Resonance* (S. Geschwind, ed.), Plenum Press, New York (1972), p. 263.

³³⁾J. Jackle, *Z. Phys.* **257**, 212 (1972).

³⁴⁾A. K. Przhvuskiĭ, in: *Spektroskopiya Kristallov (Crystal Spectroscopy)*, Nauka, Leningrad (1983), p. 82.

Translated by A. Mason